

High Sensitive Microwave Microfluidic Sensor Based on Split Ring Resonator for Determination Liquid Permittivity Characterization

Ahmed Adnan Al-Mudhafar¹, Ali A. Abduljabar², Hayder Jawad Albattat¹

¹ Department of Communication Technologies Engineering, Engineering Technical College, Al-Furat Al-Awsat Technical University, 31001, Najaf, Iraq.

² Department of Electrical Engineering, College of Engineering, University of Basrah, 61001 Basrah, Iraq

E-mail: ahmedadnan_ahmedadan@yahoo.com

E-mail: aliaiq76@gmail.com

E-mail: hayder.albattat@atu.edu.iq

<https://dx.doi.org/10.46649/300320-02>

Abstract— a microwave microfluidic microstrip split ring resonator is presented in this paper for liquid sensing and characterization. The sensor is designed to operate at frequency of 1.4 GHz and quality factor of 360. The sensor has been tested with several solvents to verify its sensitivity where the resonant frequency and losses vary with each solvent. The shift in the resonant frequency and the change in the insertion loss have been used to extract the values of the complex permittivity of the solvent. The measured complex permittivities of the solvents have been compared with the theoretical values with very good agreement. This sensor can be utilized in many industrial and medical application where the characterization of liquids are needed.

Keywords— Complex permittivity ,split ring resonator, liquids.

I. INTRODUCTION

Microwave resonators are commonly used as precise instruments for measurements of dielectric and electromagnetic properties of materials such as the complex permeability and complex permittivity and surface resistance at microwave frequencies. In [1] they can also be applied as chemical, humidity sensor or paramagnetic impurities sensor.

In the recent years, the integration of microfluidic structure with microwave has resulted very attractive characteristics and enable label-free, real time monitoring of Escherichia coli bacteria [2], glucose concentration [3] and growth of pathogenic bacteria [4], detect saline in biological range [5], chemical sensing application [6] [7], and dielectric characterization of microparticles which can be adapted for single cell investigations in medical and biological applications[8]. Microfluidic sensor for measurement of complex permittivity of mixture liquid, such as water and ethanol with respect to frequency resonator and high-Q using split ring resonator is presented in [9] while [10] is based on the changes in peak attenuation and frequency resonator. Measurements of dielectric property, size, speed, and the liquid segments are proposed in [11] while the correction of liquid permittivity measurements due to the temperature effect is suggested in [12] [13].

Perturbation theory can be used to measure of complex permittivity for liquids with respect to frequency resonator and quality factor of sensor [14]. Recently, split ring resonator (SRR) enables to sense different types of liquids using capillary or microfluidic channel (microfluidics deals with very precise fluid control, under small volumes and size) [15].

In this paper, a low cost and lightweight split ring resonator inside cylindrical cavity has been designed and fabricated as high sensitive microfluidic sensor for measuring the characterization of pure liquid (water, ethanol, and chloroform) at 1.434 GHz with 0.4 nL effective volume. In section (II) the theory and concept are illustrated. In section (III) the description of the sensor design and fabrication is presented. Section (IV) experimental results. Finally the conclusions are drawn in section (V).

II. THEORY AND CONCEPT

A. RESONANCE PERTURBATION

Cavity resonators is perturbed by introducing a small piece of dielectric so one of its applications is to determine the complex permittivity of the sample by measuring the shift in the resonant frequency and the change in the quality factor due to changes in material properties of cavity [16]. If the material is lossless, dielectric constant

(ϵ') of sample can be calculated from shift in resonant frequency [17].

In the presence of, gap (slit) at this case the ring resonator called split ring resonator, where two microstrip lines are in parallel with a separation distance (d) this lines support two modes as shown in Fig.1.(a) odd mode it can be seen the positive maximum electric field point (+) and negative maximum electric field point (-) at slit (opposite voltage sign) resulting electric wall and Fig.1.(b) even mode it can be seen the positive maximum electric field point (+) at both side of slit (same voltage sign) resulting magnetic wall [18].

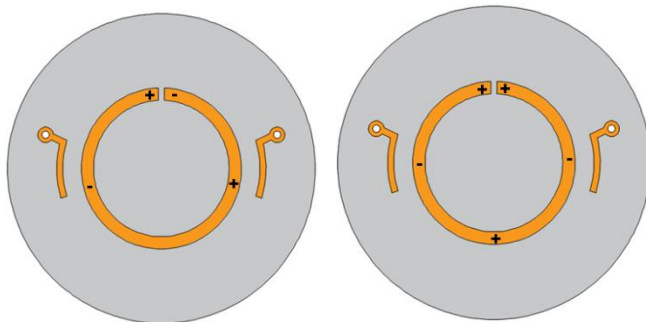


Fig.1 Maximum field point for the first two points.(a) first mode.(b) second mode

A $\lambda/2$ open-circuited microstrip SRR coupled to the two open end of symmetric a microstrip transmission feed lines in which both the input and output impedance are Z_0 , the symmetric feed lines are positioning at a magnetic field antinode were used to excite the split ring by inductive couplings with a smaller degree of capacitive coupling [14] as depicted in the Fig.1. The gap can be modeled as a series capacitors and as parallel inductors between the resonator and the microstrip line, so the equivalent circuits can be constructed as shown in Fig.2.

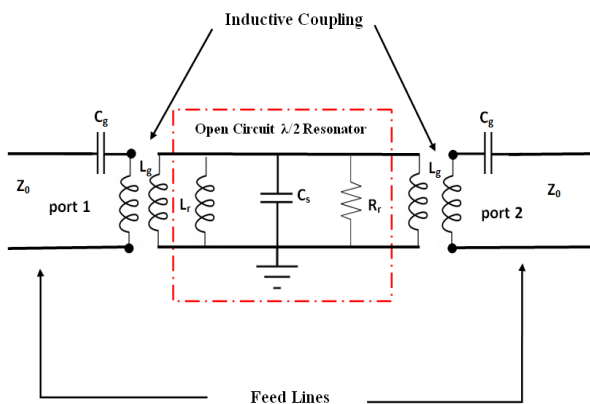


Fig.2 Equivalent circuit of split ring resonator (SRR)

Where the coupling inductive with capacitance between the feed line and split ring is denoted by L_g C_g respectively, C_s is the capacitance of slit in the ring, lossless ring resonator is expressed by L_r in addition losses ring resonator is expressed by R_r , then frequency resonator (fr) for any mode (n is number of mode) can be found as:

$$f_r = \frac{nc}{2\pi\sqrt{(L_r+L_g)(C_g+C_s)}} \quad (7)$$

A. Debye Model

The complex permittivity of polarized liquid can be written as :

$$\epsilon = \epsilon' - j\epsilon'' \quad (8)$$

Complex dielectric constant as function of frequency derived by Debye theory [19 and 20]:

$$\epsilon(\omega) = \epsilon_\infty + \frac{\epsilon_s - \epsilon_\infty}{1 + j\omega\tau} \quad (9)$$

Where ϵ' corresponds to the real part (dielectric constant), ϵ'' to the imaginary part (loss factor), $\omega = 2\pi f_r$, τ is relaxation time constant, ϵ_s is the static permittivity (i.e. if the frequency of the variable field tends to zero), and ϵ_∞ is the high frequency permittivity (i.e. the value of (ω) at infinite frequency).

III. FABRICATION OF THE SENSOR

The SRR is used here as microwave microfluidic sensor to measure complex permittivity of liquids designed based on papers [8, 11, 14, 21].

TABLE I

DIMENSIONS OF SENSOR (mm)

r1	r2	r3	r4	r5	r6	r7	l	g	d
25	17	16	13	11	1.2	0.65	9	1	0.5

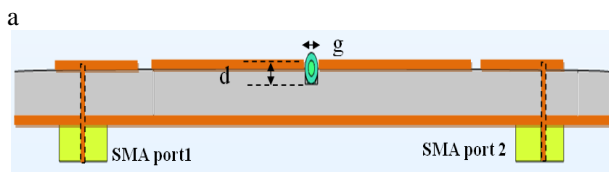
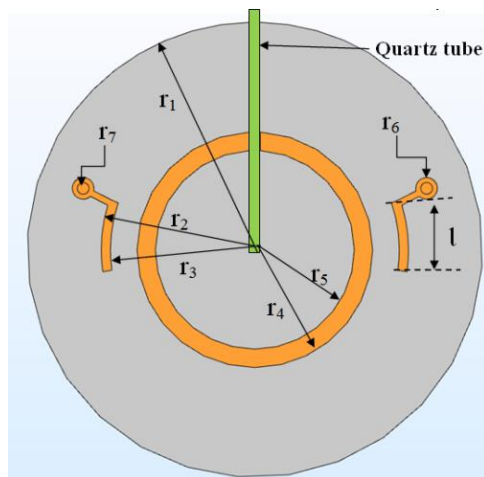


Fig.3 Schematic of the sensor which consists of split ring resonator with quartz tube .(a) Top view,(b) Side view.

The SRR is fabricated using Rogers corporation RT/duroid 5870 laminate (Rogers Corporation, USE) with thickness of copper is $35\mu\text{m}$, conductivity of copper is $2.7 \times 10^7\text{S/m}$, dielectric thickness is 1.57 mm, relative permittivity of 2.33 ± 0.02 , and loss tangent 0.0012. SMA connectors with 50Ω used as input and output port of the resonator. A quartz glass tube was used as microfluidic channel with outer diameter 1mm and inner diameter 0.5mm and relative permittivity 3.8. Geometric shapes and dimensions of the SRR are shown in Fig.3 and Table 1 respectively.

High electric field distribution is at edge of ring gap so the introducing of the quartz tube into the ring gap will polarize the liquid inside the gap. And the sensor is packaged inside an aluminum cylindrical cavity to increase the quality factor from 310 to 360 when loaded with empty tube by reducing dissipated loss. Fig.4.(a) shows the sensor structure with cavity's dimension. The SMA coaxial feeding ports are designed in the button of the microstrip where two holes are made in the cylindrical cavity button as shown in the Fig.4.(b). The groove was made on the microstrip upper surface passing through the ring gape where the capillary is put as shown in Fig.4 (c), the capillary passes the cavity wall through the hole which gives the ability to fill the capillary from outside the cavity .

IV. EXPERIMENTAL RESULTS AND DISCUSSION

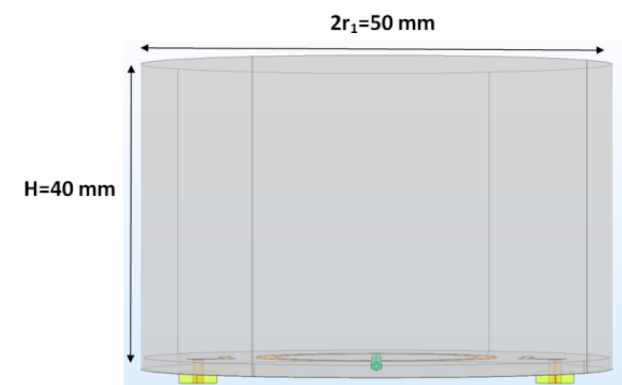
Fig.5 shows the system design used in this section. Small and thin capillary quartz glass tubes transparent

color with outside diameter 1 mm has been used as microfluidic channel carries liquid sample depends on the physical phenomenon called capillary action. A portable vector network analyzer (VNA- KC901V) used to measure the change in the in insertion loss, and finally micropipette (NEXTY-1000) to prepare mixtures of water - ethanol with different percentages, which will be explained in detail in the next sections.

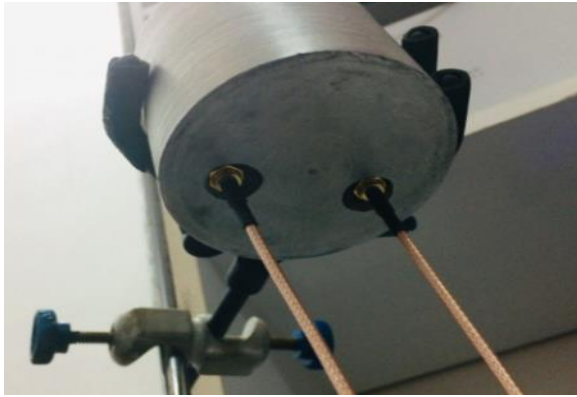
A. Pure Liquid's Characteristics

Frequency response was recorded from (1.425-1.44) GHz , the transmission coefficient (S_{21})was measured at frequency resonator with empty tube and when it was filled with common solvents, all these measurements were taken at room temperature 25°C . Several solvents have tested such as water, ethanol, and chloroform and the results are shown in Fig.6. Table 2 shows the extracted information from the Fig 6 such as the shift in resonant frequency and the change in the insertion loss which have been used to calculate the Debye Model parameters as shown in Fig 6. Also the theoretical values of the Debye model have been presented in Table two to compare with the measured results.

Here, the measurement with empty tube is considered as reference to compute percentage shift in resonance frequency of the sensor when the tube loaded with solvents, these percentages have been plotted as functions of real part of complex permittivity as shown in Fig.7 We shows from that plot the shift in frequency decrease with decreasing dielectric constant (ϵ') (give an approximately linear dependence on the real part of complex permittivity).



a



b



c

Fig.4 (a) Schematic of the sensor inside the cavity with its dimensions.(b)Photograph of the cylindrical cavity holes with coaxial feeding(c) Photograph of the fabricated cylindrical cavity, sensor and tube inside it.

This section is dedicated to extract the mathematical model which is used to evaluate the complex permittivity of water-ethanol mixtures with a ratio of 10% up to 100% using SRR.

At the first point, mixture of water-ethanol has been prepared with ration of 20% up to 100%, the value of the of step 20% to achieve the effect of complex permittivity on SRR characteristics, so that each mixture is 1mL using micropipette to prepare the mixtures. , the complex permittivity of water- ethanol mixtures are taken from [22] and at each step the resonance frequency and insertion losses of sensor are measured, the mathematical model is evaluated from the shift in the resonance frequency as well as the change in maximum attenuation $|S_{21}|$ as function of complex permittivity which can be expressed in matrix form [23]:

$$\begin{bmatrix} \Delta fr \\ \Delta |S_{21}| \end{bmatrix} = \begin{bmatrix} q_1 & q_2 \\ q_3 & q_4 \end{bmatrix} \begin{bmatrix} \Delta \epsilon' \\ \Delta \epsilon'' \end{bmatrix} \quad (10)$$

Where

$$\Delta \epsilon' = \epsilon'_{\text{sample}} - \epsilon'_{\text{reference}}, \Delta \epsilon'' = \epsilon''_{\text{sample}} - \epsilon''_{\text{reference}}, \Delta fr = fr_{\text{sample}} - fr_{\text{reference}}, \text{ and } \Delta |S_{21}| = |S_{21}|_{\text{sample}} - |S_{21}|_{\text{reference}}.$$

Consider the reference sample as the mixture 100% water fraction (w100%). All of these measurements are listed in Table3.

Matrix can be determined by same method explained in [23]:

$$\begin{bmatrix} \Delta fr \\ \Delta |S_{21}| \end{bmatrix} = \begin{bmatrix} -0.000011 & 0.000139 \\ 0.005257 & 0.145272 \end{bmatrix} \begin{bmatrix} \Delta \epsilon' \\ \Delta \epsilon'' \end{bmatrix} \quad (11)$$

Mathematical model used to measure the complex permittivity related to change in (fr and $|S_{21}|$) from take inverse matrix (equation (11)) can be written as equation :

$$\Delta \epsilon' = -63693.84 \Delta fr + 60.92 \Delta |S_{21}| \quad (12)$$

$$\Delta \epsilon'' = 2305.04 \Delta fr + 4.68 \Delta |S_{21}| \quad (13)$$

The same results as the mixtures of water and ethanol in ratios of 20% to 100%, were used to validate the equations (12) and (13) and measurement recorded also in Table3. Fig.8.Comparison between measured and literature value for water fraction volume changing from 20% to 100% with step values 20% (a) real part of complex permittivity (b) imaginary part complex permittivity. Through the last two figures (Fig. (a) and (b)) the results show, good agreement between measured (extracted from the equations (12) and (13)) and theoretical values of the liquids complex permittivity so that an acceptable accuracy of mathematical model is higher than 93.34% .

To verify presented sensor model, we again prepare mixtures of water and ethanol in random ratios such as (10%,25%,50%, and 95%) and at each ratio measure the resonance frequency maximum attenuation peak of the sensor together with compute the difference in the real part, and imaginary part of complex permittivity from simplified model equations ((12) and (13)) and determine the dielectric constant(ϵ') and loss factor (ϵ'') for these sets of sample with respect to the reference sample (w100%) also all these measurements were taken at laboratory temperature 25°C and listed in Table 4. Fig.9 Show the frequency resonator of SRR and S_{21} are varied with different water fraction volume and show the frequency resonator decrease with increasing concentration of water and insertion loss decrease with decrease concentration of water.

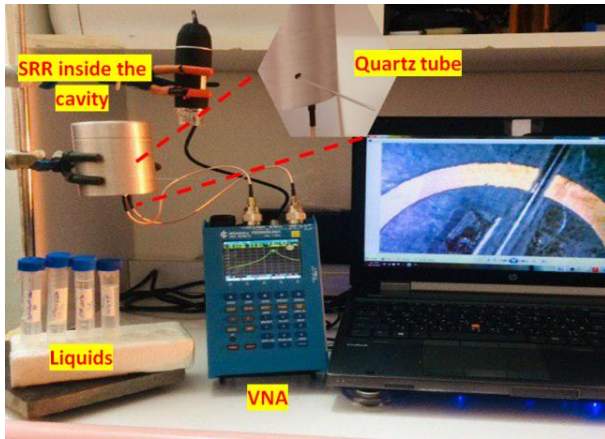


Fig.5 Experimental configuration

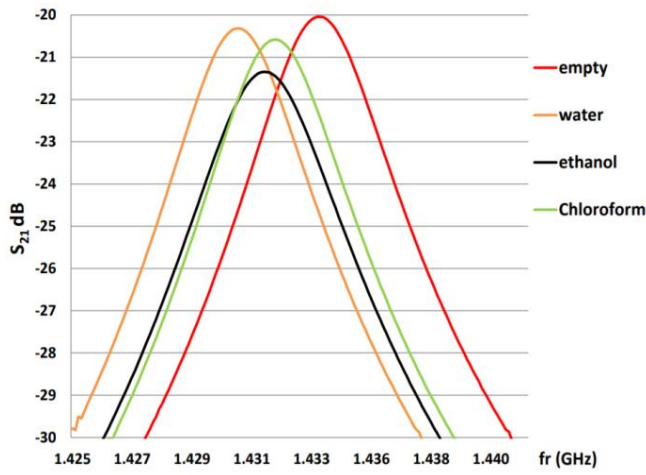


Fig. 6 Measured S_{21} of the sensor using quartz tube at resonant frequency

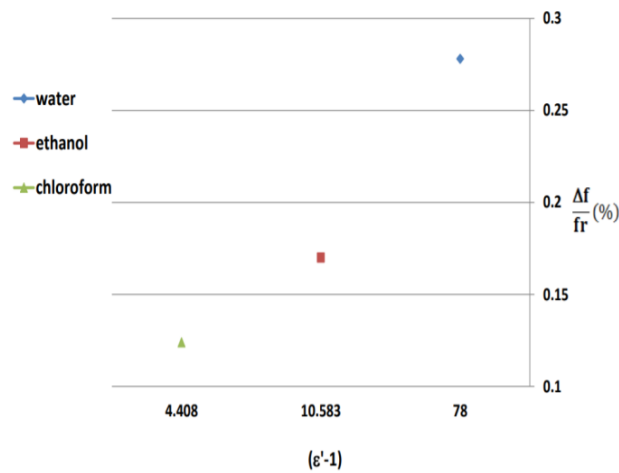


Fig.7 Percentage change in center frequency with respect to permittivity of measured liquids

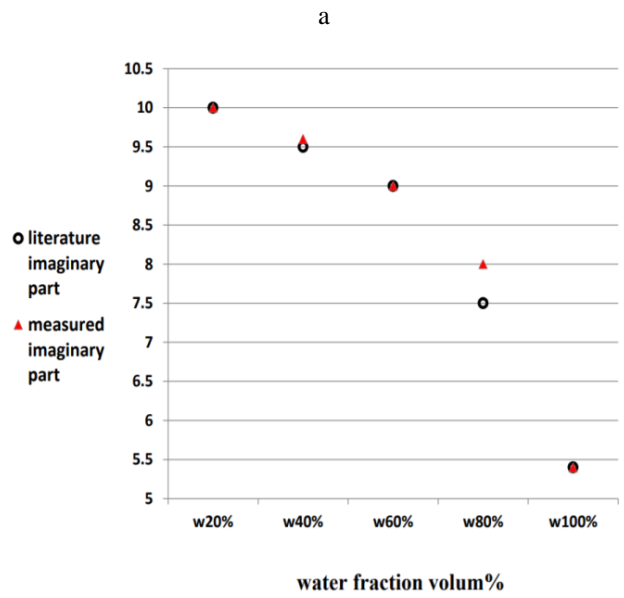
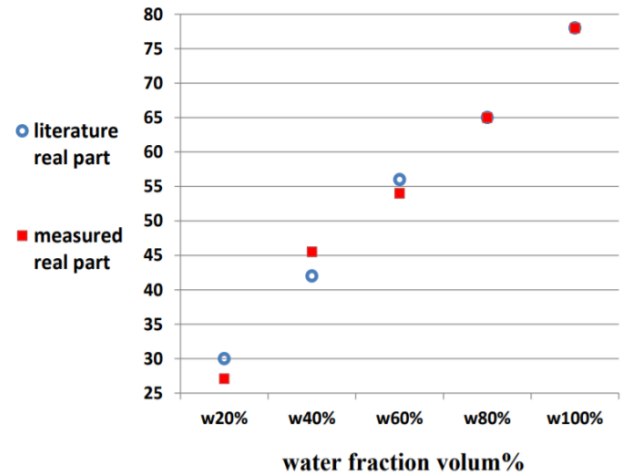


Fig.8 Measured and literature value for water fraction volume changing from 20% to 100% with step values 20% (a) real part . and (b) imaginary part of complex permittivity.

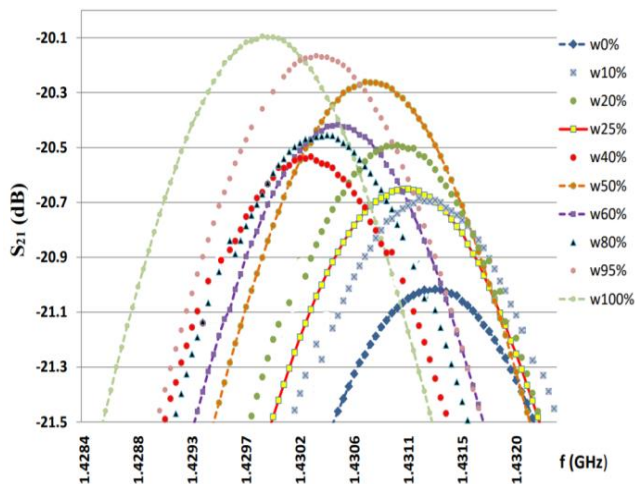


Fig.9 Measured changes in the frequency resonator and S_{21} of SRR are varied with different water fraction volume changing from 10% to 100% .

Fig.10 shows relation between dielectric constant (real part of complex permittivity) and dielectric losses (imaginary part of complex permittivity) with increase water fraction volume. these results are expected because when water-ethanol mixture fraction Volume increase from 10% to 100% real part(ϵ') increases, shift in frequency resonator decrease and frequency resonator of SRR is increasing. also, when water-ethanol mixture fraction volume increase from 10% to 100% imaginary part(ϵ'') decreases, a loss is decreasing. We notice that with different water volume fraction is changed from 0% to 100%, the frequency and resonance of resonance characterizations change dramatically although the effective fluid volume is approximately very small 0.4 nL.

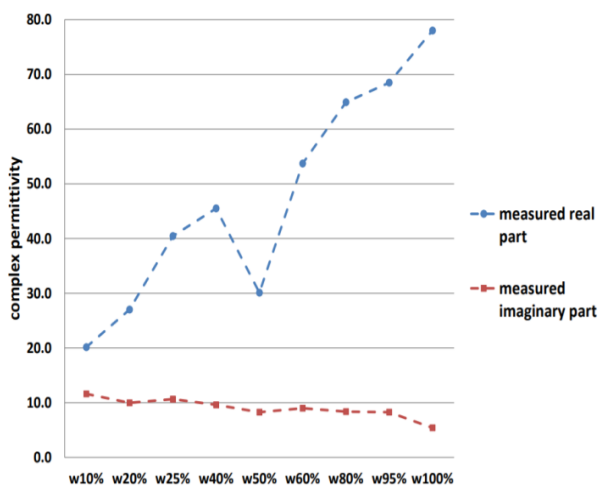


Fig.10 Relation between dielectric constant (real part of complex permittivity) and dielectric losses(imaginary part of complex permittivity) with increase water fraction volume.

V. CONCLUSIONS

In this paper a new microwave microfluidic sensor was designed using microstrip split ring resonator. The sensor

operates at frequency of 1.4 GHz with quality factor of 360. The application of the sensor is to characterize liquid complex permittivity with small volume of 0.4 nL. The sensor has been test with several solvents as well as water-ethanol mixture. The results show a well arrangement between the measured and theoretical values of the liquids complex permittivity so that the accuracy is higher than 93.34% .

REFERENCES

- [1] . Mazierska, J. Krupka, M. Bialkowski, M. V. Jacob, *Microwave Resonators and Their Use as Measurement Instruments and Sensors*, Third IEEE Int. Workshop on Electronic Design Test and Applications, (2006).
- [2] S. Mohammadi, R. Narang, M. MohammadiAshani, H. Sadabadi, A. Sanati-Nezhad, and M. H. Zarifi, *Real-time monitoring of escherichia coli concentration with planar microwave resonator sensor*, *Microw. Opt. Technol. Lett.*, Jun. (2019)
- [3] Mondal, D., N. K. Tiwari, and M. J. Akhtar, *Microwave assisted non-invasive microfluidic biosensor for monitoring glucose concentration*, *Proceedings of IEEE Sensors*, Vol. 2018, Oct.(2018).
- [4] Narang, R.; Mohammadi, S.; Ashani, M.M.; Sadabadi, H.; Hejazi, H.; Zarifi, M.H.; Sanati-Nezhad, A, *Sensitive, real-time and non-intrusive detection of concentration and growth of pathogenic bacteria using microfluidic-microwave ring resonator biosensor*, *Sci. Rep.* 2018, 8, 15807 (2018)
- [5] Kilpijärvi, J.; Halonen, N.; Juuti, J.; Hannu, J, *Microfluidic microwave sensor for detecting saline in biological range*, *Sensors* 19, 819,(2019).
- [6] Salim, A, Ghosh, S and Lim, S, *Low-cost and lightweight 3d-printed split-ring resonator for chemical sensing applications*, *Sensors* 18, 3049, (2018) .
- [7] A. Salim and S. Lim, *Complementary split-ring resonator-loaded microfluidic ethanol chemical sensor*, *sensors*, vol. 16, pp. 1-13, (2016).
- [8] Ali A. Abduljabar, X. Yang, D. Barrow, A. Porch, *Microstrip split ring resonator for microsphere detection and characterization*, *Proc/ IEEE MTT-S Int. Microw.Symp. Dig. (IMS)*, pp. 1-4, (2015)-May-17-22.
- [9] W. Withayachumnankul, K. Jaruwongrungrsee, A. Tuantranont, C. Fumeaux, D. Abbott, *Metamaterial-based microfluidic sensor for dielectric characterization*, *Sens. Actuators A Phys.*, vol. 189, pp. 233-237, Jan, (2013).
- [10] A. Ebrahimi, W. Withayachumnankul, S. Al-Sarawi, D. Abbott, *High-sensitivity metamaterial-inspired sensor for microfluidic dielectric characterization*, *IEEE Sensors J.*, vol. 14, no. 5, pp. 1345-1351, May (2014).
- [11] Ali A.Abduljabar, A. Porch, D. A. Barrow, *Real-time measurements of size speed and dielectric property of liquid segments using a microwave microfluidic sensor*, *IEEE MTT-S International Microwave Symposium (IMS2014)*, pp. 1-4, (2014).
- [12] Ali A. Abduljabar, N. Clark, J. Lees, A. Porch, *Dual mode microwave microfluidic sensor for temperature variant liquid characterization*, *IEEE Trans. Microw. Theory Techn.*, vol. 65, no. 7, pp. 2572-2582, Jul. (2017).
- [13] Ali A. Abduljabar, H. Hamzah, A. Porch, *Double microstrip microfluidic sensor for temperature correction of liquid characterization*, *IEEE Microw. Wireless Compon.Lett.*, vol. 28, no. 8, pp. 735-737, Aug, (2018).
- [14] Ali A. Abduljabar, D. J. Rowe, A. Porch, D. A. Barrow, *Novel microwave microfluidic sensor using a microstrip split-ring resonator*, *IEEE Trans. Microw. Theory Techn.*, vol. 62, no. 3, pp. 679-688, Mar, (2014).
- [15] O. Korostynska, A. Mason, and A. I. Al-Shalman'a, *Flexible microwave sensors for real-time analysis of water contaminants*, *1.Electromagn.Waves Appl.*, vol. 27, no. 16, pp. 2075-2089, Nov. (2013).
- [16] D. M. Pozar, *Microwave Engineering*, Fourth Edition Wiley, (2012).

- [17] Ida, N., *Open Resonator Microwave Sensor Systems For Industrial Gauging*, A practical design approach. London, IET (2018).
- [18] K. Chang, L. H. Hsieh, *Microstrip Ring Circuits and Related Structures*, New York:Wiley, (2004).
- [19] P. Debye, *Polar Molecules*, The Chemical Catalog, New York, (1929).
- [20] F. Buckley and A. A. Maryott, *Tables of Dielectric Dispersion Data For pure Liquids and Dilute Solutions*, Nat. Bureau Standards Circular, vol.589, p. 6, Nov. (1958).
- [21] Ali A. Abduljabar, X. Yang, D. A. Barrow, A. Porch, *Modelling and measurements of the microwave dielectric properties of microspheres*, IEEE Trans. Microw. Theory Techn., vol. 63, no. 12, pp. 4492-4500, Dec. (2015).
- [22] J.-Z. Bao, M. L. Swicord, and C. C. Davis, *Microwave dielectric characterization of binary mixtures of water, methanol, and ethanol*, J. Chem. Phys., vol. 104, no. 12, pp. 4441-4450, (1996).
- [23] W. Withayachumnankul, K. Jaruwongrunsee, A. Tuantranont, C. Fumeaux, and D. Abbott, *Metamaterial-based microfluidic sensor for dielectric characterization*, Sens. Actuators A, Phys., vol. 189, pp. 233-237, Jan. (2013).

TABLE II

MEASUREMENTS OF COMPLEX PERMITTIVITY OF COMMON LIQUIDS AT RESONANT FREQUENCY AND ROOM TEMPERATURE 25°C

liquids	Literature [20]				measured				
	ϵ_s	ϵ_∞	τ (ps)	f_r (GHz)	ϵ'	ϵ''	ϵ	IL (dB)	$\frac{\Delta f}{f_r}$ (%)
empty	1	1	----	1.43377	1	0	1	20	----
water	78.4	5.16	8.27	1.4298	78	5.4	78-j5.4	20.1	0.278
ethanol	24.3	4.2	163	1.43133	10.583	9.357	10.583-j9.357	21.02	0.170
chloroform	4.72	2.5	7.96	1.432	4.408	0.1582	4.408-j0.1582	20.1	0.124

TABLE III

A COMPARISON OF THE COMPLEX PERMITTIVITY OF LITERATURE AND MEASURED VALUES AT 1.43 GHz AND 25°C OF WATER - ETHANOL MIXTURES AT CONCENTRATIONS VARYING FROM 20% TO 100% WITH THE STEP SIZE 20%

volume fraction of water	Literature [22]						measured					
	ϵ'	ϵ''	ϵ	$\Delta\epsilon'$	$\Delta\epsilon''$	f_r (GHz)	$ S_{21} $ (dB)	Δf_r	$\Delta S_{21} $	ϵ'	ϵ''	ϵ
w20%	30	10	30-j10	-48	4.6	1.43098	20.49	0.00118	0.3969	27.1	10.0	27.1-j10
w40%	42	9.5	42-j9.5	-36	4.1	1.43073	20.53	0.00093	0.4390	45.5	9.6	45.5-j9.6
w60%	56	9	56-j9	-22	3.6	1.43049	20.42	0.00069	0.3225	54	9	54-j9
w80%	65	7.5	65-j7.5	-13	2.1	1.43035	20.46	0.00055	0.3600	65	8	65-j8
w100%	78	5.4	78-j5.4	0	0.0	1.42980	20.10	0.00000	0.0000	78	5.4	78-j5.4

TABLE IV

MEASURE COMPLEX PERMITTIVITY OF AT 1.43 GHz AND 25°C OF WATER - ETHANOL MIXTURES AT DIFFERENT WATER CONCENTRATIONS

Volume fraction of water	f_r (GHz)	$ S_{21} $ (dB)	Δf_r	$\Delta S_{21} $	$\Delta\epsilon'$	$\Delta\epsilon''$	ϵ'	ϵ''	ϵ
w10%	1.43128	20.69	0.00148	0.5978	-57.849	6.209	20.2	11.6	20.2-j11.6
w25%	1.43093	20.66	0.00113	0.56510	-37.548	5.249	40.5	10.6	40.5-j10.6
w50%	1.43071	20.26	0.00091	0.1650	-47.910	2.870	30.1	8.3	30.1-j8.3
w95%	1.4303	20.46	0.00050	0.3666	-9.514	2.868	68.5	8.3	68.5-j8.3